Analysis of Laminar Non-Newtonian Flow and Heat Transfer in Curved Tubes

The governing equations for the laminar fully developed flow and heat transfer in curved tubes are solved numerically for a power-law fluid. Results for the velocity and temperature fields, the friction factor, and the Nusselt number are presented for different values of the Dean number, the Prandtl number, and the power-law index. The friction factor results are compared with available experimental data.

CHIA-FU HSU and S. V. PATANKAR

Department of Mechanical Engineering
University of Minnesota
Minneapolis, MN 55455

SCOPE

Curved tubes are often used in different types of process equipment. The study of flow and heat transfer in such tubes is required for the proper design of the corresponding equipment. Although the Newtonian flow in curved tubes has been extensively analyzed, there appears to be little theoretical work on the non-Newtonian flow in curved tubes. Some experimental data for the friction factor in curved tubes have been reported by Rajasekharan et al (1970), Gupta and Mishra (1974), Mashelkar and Devarajan (1976b), and Mujawar and Rao (1978). For the heat transfer in curved tubes, no theoretical or experimental study seems to have been undertaken.

The objective of the present paper is to provide numerical solutions of the differential equations that govern the laminar fully developed velocity and temperature fields of a power-law fluid flowing in a curved tube. The governing equations are written in appropriate dimensionless form to identify the independent parameters of the problem. The numerical results are presented for a range of the values of these parameters.

CONCLUSIONS AND SIGNIFICANCE

For large radius of curvature, the non-Newtonian flow is governed by the power-law index and by the modified Dean number. The heat transfer is additionally governed by the Prandtl number. The axial velocity profiles are distorted by the centrifugal force, although they tend to be flatter for lower values of the power-law index. The secondary flow in the tube cross section exhibits an interesting boundary layer behavior, especially at high Dean numbers. The friction factor increases with the Dean number and also with the power-law index. The computed values of the friction factor are compared with experimental data and the agreement is very satisfactory.

The overall heat transfer coefficient also increases with the Dean number. Indeed, the increase in the heat transfer coefficient is more pronounced than that in the friction factor. Thus, a curved tube appears to be an attractive device for heat transfer enhancement for all the values of the power-law index considered.

The local heat transfer coefficient varies significantly over the circumference of the tube for low Prandtl numbers. The heat transfer coefficient becomes more uniform as the Prandtl number increases.

It can be concluded that reliable numerical solutions can now be obtained for this complex flow problem. The presented results should be useful to the designers of process equipment involving non-Newtonian flow in curved tubes.

BACKGROUND

Curved tubes in the form of helical or spiral coils are frequently used in many engineering applications to enhance the processes of heat and mass transfer. The enhancement occurs due to the existence of a secondary flow, which appears as twin counter-rotating vortices in the cross-sectional plane.

For a Newtonian fluid, the flow in curved tubes has been extensively investigated. For the flow in a round curved tube, Dean (1927) solved the Navier-Stokes equations analytically for tubes with large radius of curvature. He discovered that the secondary flow could be characterized by a dimensionless number, later called the Dean number, which is the ratio of the Reynolds number to the square-root of the dimensionless radius of curvature. Other theoretical investigations of the fully developed flow of a Newtonian fluid in a round curved tube are reported by Topakoglu (1967), McConalogue and Srivastava (1968), Truesdell and Adler (1970), Akiyama and Cheng (1971), Austin and Seader (1973), and Patankar, Pratap and Spalding (1974).

The *non-Newtonian* flow in curved tubes, on the other hand, has not been analyzed to the same extent. The only available analysis appears to be that of Mashelkar and Devarajan (1976a), who solved the momentum equations for the laminar flow of a power-law fluid in curved tubes using a boundary layer approximation. Their results, therefore, are applicable only at high Dean numbers, for which the secondary flow exhibits a boundary layer character.

Experimental data and empirical correlations for the friction factor in curved tubes for various power-law fluids have been reported by Rajesekharan, Kubair, and Kuloor (1970), Gupta and Mishra (1974), Mashelkar and Devarajan (1976b), and Mujawar and Rao (1978). The available data will be reviewed later in this paper, and some data will be used for comparison with the theoretical results of the present work.

Correspondence concerning this paper should be addressed to S. V. Patankar.
0001-1541-82-6096-0610 $2.00.

The aforementioned experimental studies report only the friction factor. Little information is available about the axial velocity profile or the secondary flow. Further, the enhancement of heat transfer, which is the most important characteristic of the flow in curved tubes, has not been studied for non-Newtonian flows—either experimentally or theoretically.

The purpose of the present work is to provide numerical solutions for the fully developed flow and heat transfer for a power-law fluid flowing in a curved tube. The tube radius is assumed to be small in comparison with the radius of curvature. The governing differential equations for the flow and heat transfer are solved by the numerical method described in Patankar (1980).

ANALYSIS

A schematic representation of a curved tube is shown in Figure 1. The toroidal geometry there is a good approximation for a helically coiled tube of small pitch. The coordinate system appropriate for this configuration is the orthogonal curvilinear system r, θ, ϕ shown in Figure 1.

Since the flow is considered to be fully developed, the velocity components are independent of ϕ. The quantity that changes with ϕ is the pressure p, which decreases linearly with ϕ. Indeed, the pressure gradient $(1/R)\,(\partial p/\phi\partial)$, denoted here by P_ϕ is constant for the fully developed flow and determines the amount of the throughflow in the coil.

Equations of Motion. If the tube radius a is considered to be small in comparison with the coil radius R, the equations of motion in the r, θ, ϕ coordinates are nearly the same as those in the polar coordinates, r, θ, z. The only difference is that, for the r, θ, ϕ system, the components of the centrifugal force $\rho u_\phi^2/R$ appear in the momentum equations for the r and θ directions. For the non-Newtonian flow, the apparent viscosity μ is not constant; a reference viscosity μ_{ref} is, therefore, used to nondimensionalize the variables.

The dimensionless variables are defined as follows.

$$\eta = r/d \tag{1a}$$

$$U_r = \rho u_r d/\mu_{\text{ref}}, \qquad U_\theta = \rho u_\theta d/\mu_{\text{ref}} \tag{1b}$$

$$U_\phi = u_\phi \mu_{\text{ref}}/(d^2 P_\phi) \tag{1c}$$

$$P = p\rho d^2/\mu_{\text{ref}}^2 \tag{1d}$$

$$M = \mu/\mu_{\text{ref}} \tag{1e}$$

The resulting dimensionless forms of the equations of motion are:

continuity

$$\frac{1}{\eta}\frac{\partial}{\partial \eta}(\eta U_r) + \frac{1}{\eta}\frac{\partial U_\theta}{\partial \theta} = 0 \tag{2}$$

r-direction momentum

$$U_r\frac{\partial U_r}{\partial \eta} + \frac{U_\theta}{\eta}\frac{\partial U_r}{\partial \theta} - \frac{U_\theta^2}{\eta} = -\frac{\partial P}{\partial \eta} + \nabla\cdot M\nabla U_r - \frac{M}{\eta^2}\left(2\frac{\partial U_\theta}{\partial \theta} + U_r\right) + S_{cr} + S_{vr} \tag{3}$$

θ-direction momentum

$$U_r\frac{\partial U_\theta}{\partial \eta} + \frac{U_\theta}{\eta}\frac{\partial U_\theta}{\partial \theta} + \frac{U_r U_\theta}{\eta} = -\frac{1}{\eta}\frac{\partial P}{\partial \theta} + \nabla\cdot M\nabla U_\theta + \frac{M}{\eta^2}\left(2\frac{\partial U_r}{\partial \theta} - U_\theta\right) + S_{c\theta} + S_{v\theta} \tag{4}$$

ϕ-direction momentum

$$U_r\frac{\partial U_\phi}{\partial \eta} + \frac{U_\theta}{\eta}\frac{\partial U_\phi}{\partial \theta} = 1 + \nabla\cdot M\nabla U_\phi \tag{5}$$

Here the operator $\nabla\cdot M\nabla$ is defined as

$$\nabla\cdot M\nabla = \frac{1}{\eta}\frac{\partial}{\partial \eta}\left(\eta M\frac{\partial}{\partial \eta}\right) + \frac{1}{\eta^2}\frac{\partial}{\partial \theta}\left(M\frac{\partial}{\partial \theta}\right) \tag{6}$$

The terms S_{cr} and $S_{c\theta}$ represent the influence of the centrifugal force resulting from the flow along a curved path. They are given by:

$$S_{cr} = 2(U_\phi/\overline{U}_\phi)^2\,\text{De}^2\cos\theta \tag{7}$$

$$S_{c\theta} = -2(U_\phi/\overline{U}_\phi)^2\,\text{De}^2\sin\theta \tag{8}$$

The quantity $\overline{U}_\phi$ is the cross-sectional mean value of U_ϕ; $\overline{U}_\phi$ can be related to the mean velocity $\bar{u}_\phi$ via Eq. 1c. The Dean number De is defined as

$$\text{De} = \text{Re}\,(a/R)^{1/2} \tag{9}$$

where Re is the Reynolds number given by

$$\text{Re} = \rho\bar{u}_\phi d/\mu_{\text{ref}} \tag{10}$$

The terms S_{vr} and $S_{v\theta}$ arise from the variation of viscosity over the tube cross section. The expressions for these terms are:

$$S_{vr} = \left(\frac{\partial M}{\partial \eta}\right)\left(\frac{\partial U_r}{\partial \eta}\right) + \left(\frac{1}{\eta}\frac{\partial M}{\partial \theta}\right)\left(\frac{\partial U_\theta}{\partial \eta} - \frac{U_\theta}{\eta}\right) \tag{11}$$

$$S_{v\theta} = \left(\frac{\partial M}{\partial \eta}\right)\left(\frac{1}{\eta}\frac{\partial U_r}{\partial \theta} - \frac{U_\theta}{\eta}\right) + \left(\frac{1}{\eta}\frac{\partial M}{\partial \theta}\right)\left(\frac{1}{\eta}\frac{\partial U_\theta}{\partial \theta} + \frac{2U_r}{\eta}\right) \tag{12}$$

The boundary conditions for the equations of motion are provided simply by $u_r = u_\theta = u_\phi = 0$ at the tube wall. Because of symmetry, it is sufficient to solve the problem over only the upper semicircle of the tube cross section shown in Figure 1. The required boundary conditions along the diameter of the semicircle (i.e., for $\theta = 0$ and $\theta = \pi$) are given by $u_\theta = 0$ and $\partial u_r/\partial\theta = \partial u_\phi/\partial\theta = 0$.

It can be seen that the Dean number De is the only parameter appearing in the equations of motion, provided that the dimensionless viscosity M can expressed in terms of the other dimensionless variables. A formula for M is discussed next.

Variation of Viscosity. The apparent viscosity μ for a power-law fluid is given by

$$\mu = K[(1/2)D_{ij}:D_{ij}]^{(n-1)/2} \tag{13}$$

where n is the power-law index, K is the consistency constant, and D_{ij} is the rate of strain tensor. If, for the flow field under consideration, D_{ij} is expressed in terms of the appropriate velocity gradients, the expression for μ becomes

$$\mu = K\left[2\left(\frac{\partial u_r}{\partial r}\right)^2 + 2\left(\frac{1}{r}\frac{\partial u_\theta}{\partial \theta} + \frac{u_r}{r}\right)^2 + \left(r\frac{\partial}{\partial r}\frac{u_\theta}{r} + \frac{1}{r}\frac{\partial u_r}{\partial \theta}\right)^2 + \left(\frac{\partial u_\phi}{\partial r}\right)^2 + \left(\frac{1}{r}\frac{\partial u_\phi}{\partial \theta}\right)^2\right]^{(n-1)/2} \tag{14}$$

The corresponding reference viscosity can now be defined as

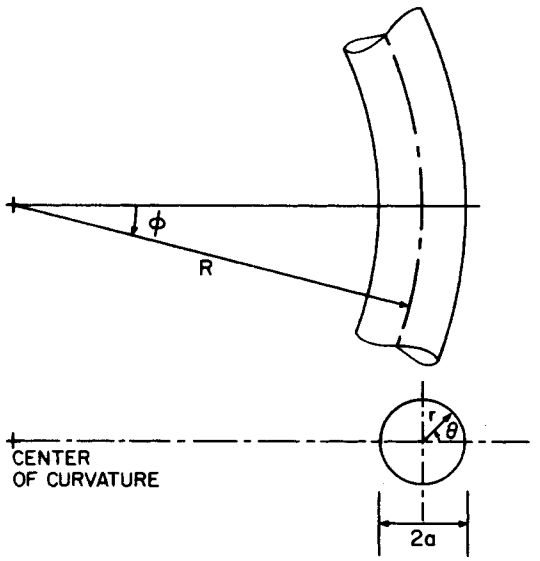

Figure 1. Geometry considered.

$$\mu_{\text{ref}} = K(\bar{u}_\phi/d)^{n-1} \tag{15}$$

If an expression for the dimensionless viscosity M is now derived from Eqs. 14 and 15, the Reynolds number Re will appear as a parameter. Then the whole problem will have De and (a/R) as two separate parameters. However, for $R \gg a$, the secondary velocities u_r and u_θ are expected to be small in comparison with the mainstream velocity u_ϕ. Therefore, the expression for M can be written as

$$M = \left[\left(\frac{\partial U_\phi}{\partial \eta}\right)^2 + \left(\frac{1}{\eta}\frac{\partial U_\phi}{\partial \theta}\right)^2\right]^{(n-1)/2} (\bar{U}_\phi)^{1-n} \tag{16}$$

which retains De as the only parameter for a given fluid. Towards the end of the paper, the effect of this approximation in the viscosity expression will be examined.

Friction Factor and Modified Parameters. If the friction factor f for the tube flow is defined by

$$f = P_\phi d \Big/ \left(\frac{1}{2}\rho \bar{u}_\phi^2\right) \tag{17}$$

it is known that, for the straight tube the product $f\text{Re}_e^+$ equals 64 for any value of the power-law index n, provided the *modified* Reynolds number Re^+ is defined as

$$\text{Re}^+ = \rho(\bar{u}_\phi)^{2-n} d^n/(CK) = \text{Re}/C \tag{18}$$

where

$$C = 8^{n-1}[(1+3n)/(4n)]^n \tag{19}$$

This implies that $C\mu_{\text{ref}}$ represents the proper characteristic viscosity for a tube flow. It, therefore, follows that the results for the curved tube should properly be based on a modified Dean number De^+ defined as

$$\text{De}^+ = \text{Re}^+ (a/R)^{1/2} \tag{20}$$

Incidentally, from Eqs. 1c, 15, 17 and 18, it can be shown that

$$f\text{Re}^+ = 2/(C\bar{U}_\phi) \tag{21}$$

Energy Equation. The heat transfer behavior is here calculated for the thermal boundary condition in which there is a uniform heat transfer rate Q' per unit length of the tube, while the wall temperature is assumed to be circumferentially uniform over any cross section. The latter assumption implies that the tube wall is made of a highly conducting material. In the thermally developed regime, the local temperature T, the wall temperature T_w, and the bulk temperature T_b all increase linearly at the same rate so that

$$\frac{\partial T}{\partial \phi} = \frac{dT_w}{d\phi} = \frac{dT_b}{d\phi} \tag{22}$$

Further, this temperature rise can be related to the heat transfer Q' via the energy balance

$$Q' = (\rho c_p \bar{u}_\phi)(\pi a^2)(1/R)(dT_b/d\phi) \tag{23}$$

A convenient dimensionless temperature is given by

$$\tilde{T} = (T_w - T)/(Q'/k) \tag{24}$$

If the fluid properties c_p and k are regarded as constants and the axial conduction and viscous dissipation are neglected, the energy equation for the thermally developed regime can now be written as

$$\text{Pr}\left(U_r \frac{\partial \tilde{T}}{\partial \eta} + \frac{U_\theta}{\eta}\frac{\partial \tilde{T}}{\partial \theta}\right) = \nabla^2 \tilde{T} + \frac{4}{\pi}\frac{U_\phi}{\bar{U}_\phi} \tag{25}$$

where

$$\nabla^2 = \frac{1}{\eta}\frac{\partial}{\partial \eta}\left(\eta \frac{\partial}{\partial \eta}\right) + \frac{1}{\eta^2}\frac{\partial^2}{\partial \theta^2} \tag{26}$$

The Prandtl number Pr appearing in Eq. 25 is defined as

$$\text{Pr} = c_p \mu_{\text{ref}}/k \tag{27}$$

in accordance with established practice. Whereas Pr is simply a *fluid* property for Newtonian fluids, it becomes a *flow* property for non-Newtonian fluids, since μ_{ref} depends on the flow velocity.

The boundary conditions for Eq. 25 are given by $\tilde{T} = 0$ at the tube wall and $\partial\tilde{T}/\partial\theta = 0$ along the diameter corresponding to $\theta = 0$ and $\theta = \pi$ in Figure 1.

For the presentation of the heat transfer results, the local heat transfer coefficient h_θ and the corresponding Nusselt number Nu_θ are defined as

$$h_\theta = q/(T_w - T_b), \qquad \text{Nu}_\theta = h_\theta d/k \tag{28}$$

where q is the local heat flux at the tube wall. The overall Nusselt number is denoted by $\overline{\text{Nu}}_c$, where the subscript c refers to the curved tube. The corresponding Nusselt number for a straight tube is denoted by $\overline{\text{Nu}}_s$. The relationship between Nu_θ and $\overline{\text{Nu}}_c$ is

$$\overline{\text{Nu}}_c = (1/\pi)\int_0^\pi \text{Nu}_\theta d\theta \tag{29}$$

The value of $\overline{\text{Nu}}_c$ can also be obtained directly from

$$\overline{\text{Nu}}_c = Q'/[\pi k(T_w - T_b)] = 1/(\pi \tilde{T}_b) \tag{30}$$

where $\tilde{T}_b$ is the dimensionless form of T_b.

RESULTS AND DISCUSSION

Computational Details. The problem formulated in the previous section was solved numerically for four values of the power-law index n; in addition to $n = 1$ (Newtonian flow), n was given the values 0.5, 0.75, and 1.25. The modified Dean number De^+ was varied from 50 to 1000. The heat transfer calculations were performed for the Prandtl number range of 1 to 1000.

The differential equations were solved by a finite-difference method. Complete details of the method are given in Patankar (1980). In the solution of the flow equations, the SIMPLER algorithm was employed. Once a converged solution for the flow field for given values of De^+ and n was obtained, it was used as an input for the solution of the energy equation, which was solved for different values of Pr.

A 17×12 grid in r-θ coordinates was used for the semicircular calculation domain. The grid spacing was uniform in the θ direction, but the r-direction spacing was chosen to be finer near the tube wall than near the tube center. Exploratory computations on finer grids and on grids of different nonuniformity indicated that the presented results are accurate to at least 0.2%. Further, the computed axial velocity profiles for $\text{De}^+ = 632.4$ and $n = 1$ were compared with the experimental data of Mori and Nakayama (1965), and the agreement was found to be very good.

Axial Velocity Profiles. A selection of the computed profiles of u_ϕ for $\text{De}^+ = 700$ is shown in Figure 2 for different values of n. The profile distortion due to the centrifugal force is in evidence in this figure. The velocity profiles tend to be flatter for the lower values of n. This is in conformity with the effect of n on the velocity profiles in a straight tube.

Secondary Velocity Profiles. Some idea of the secondary flow field can be obtained from the profiles of the circumferential velocity u_θ shown in Figure 3 for the case of $\text{De}^+ = 700$. The dimensionless variable $(u_\theta/\bar{u}_\phi)(R/a)^{1/2}$ can be shown to be equal to $U_\theta/(CD_e^+)$. Near the tube center, the circumferential velocity is seen to be uniform and rather small. Appreciable values of u_θ are found only in a region near the tube wall. This near-wall region can be regarded as a boundary layer of the secondary flow. This boundary layer originates at $\theta = 0$ and grows thicker as the secondary flow proceeds to $\theta = 180°$. The peak velocity of the secondary flow can be seen to become higher as the value of n increases.

Similar velocity profiles of the secondary flow were obtained for lower Dean numbers, except that the velocity boundary layer was thicker and the peak velocity was lower. This explains why a boundary layer analysis is inapplicable at low Dean numbers.

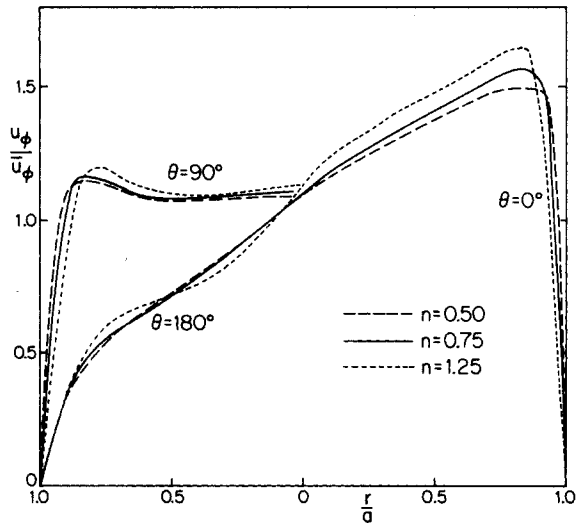

Figure 2. Axial velocity fields for different values of n presented along $\theta = 0°$, 90°, and 180° at $De^+ = 700$.

Friction Factor. Figure 4 shows the variation of f_c/f_s with De^+ for different values of n. Here the friction factors f_c and f_s are for the curved tube and the straight tube respectively. The ratio f_c/f_s can be best thought of as $(f_c Re^+)/(f_s Re^+)$, where the denominator $f_s\ Re^+$ has a constant value of 64. The curves in Figure 4 show that, for a given value of Re^+, the value of f_c increases with the Dean number and with the value of n. If a correlation for f_c/f_s is to be constructed, it follows that it should include both De^+ and n as the variables. Some of the available correlations, as will be discussed shortly, do not seem to include the influence of n.

Comparison with Experimental Data. Before the present results are compared with available experimental data, it is necessary to identify the sets of data that can be considered reliable for this purpose. As mentioned before, the data are available from four sources; they all report the values of f_c/f_s. The experimental data and the correlation given by Rajasekharan et al. (1970) imply values

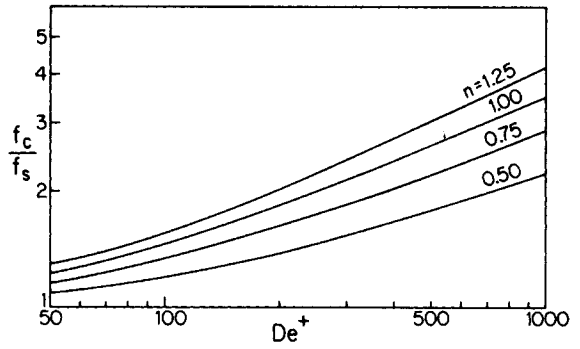

Figure 4. Variations of the friction factor ratio with the modified Dean number for different values of n.

of f_c/f_s that are about three times greater than those reported by others. The measurements of Gupta and Mishra (1975) display large scatter. Further, their f_c/f_s values are *greater* than the well-established values for Newtonian flow, although they used fluids with n values between 0.75 and 0.85. The data from these two sources are, therefore, not used for comparison here.

In Figure 5, the present results for f_c/f_s, which are shown by solid curves, are compared with the Newtonian-flow data ($n = 1$) from Ito (1970), the data from Mashelkar and Devarajan (1976b) for $n = 0.754$, and those from Mujawar and Rao (1978) for $n = 0.82$. The different data symbols refer to different values of a/R. That they seem to lie on the same curve validates the theoretical inference that a/R is not a separate parameter as long as the value of a/R is small. The agreement of the computed results with the experimental data for $n = 1$ and $n = 0.754$ can be seen to be very good. The agreement for $n = 0.82$ is also quite good at low values of De^+. In the light of the good agreement in the rest of Figure 5, the data of Mujawar and Rao (1978) at larger values of De^+ appears to be somewhat too low.

It is relevant here to comment on the empirical correlations for f_c/f_s proposed in the four papers that have reported the experimental data. The correlations of Rajasekharan et al. (1970) and Gupta and Mishra (1974) express f_c/f_s as a function of De^+ alone

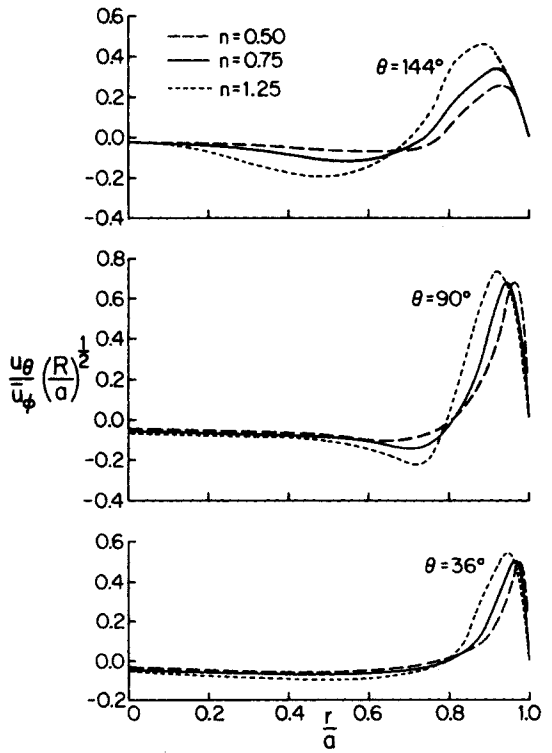

Figure 3. Velocity fields for the secondary flow for different values of n presented along three different angles at $De^+ = 700$.

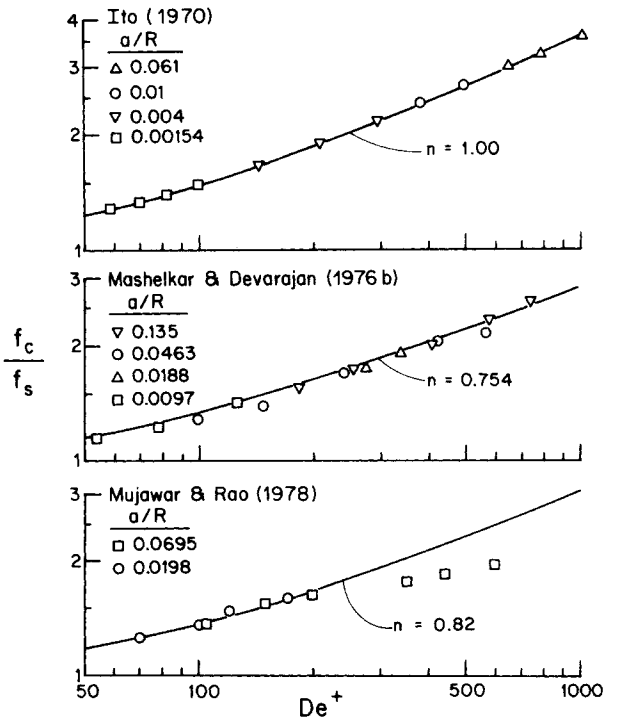

Figure 5. Comparison of the fully developed friction factor ratio with experimental data.

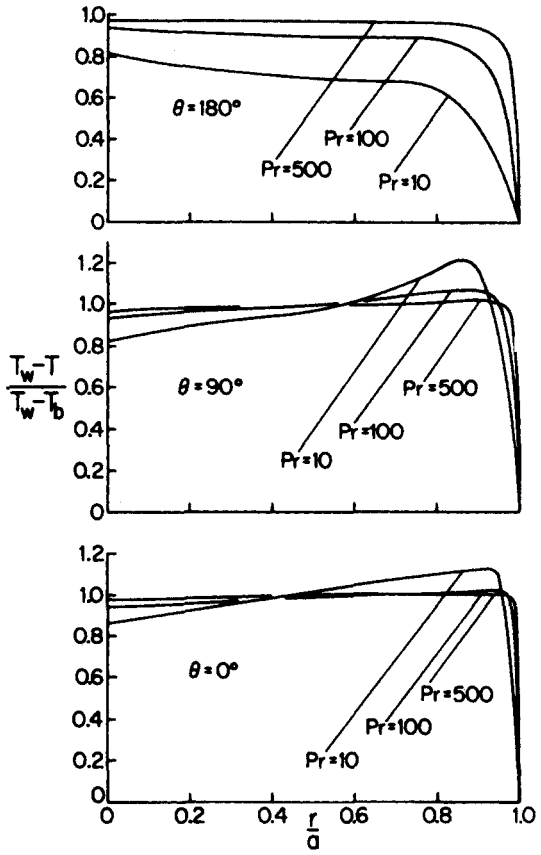

Figure 6. Temperature distribution for different Prandtl numbers presented along three different angles at $De^+ = 700$, $n = 0.75$.

and do not account for the influence of n. The correlation of Mashelkar and Devarajan (1976b) does not correctly describe the data for the *Newtonian* flow in curved tubes when n is set equal to unity. The correlation given by Mujawar and Rao (1978) does not have these obvious shortcomings. But, as indicated in Figure 5, their data and their correlation tend to underestimate f_c/f_s when De^+ is large.

Temperature Profiles. A typical set of temperature profiles are shown in Figure 6 for $n = 0.75$ and $De^+ = 700$. The temperature variation is similar to the variation of u_θ shown in Figure 3; the temperature remains uniform in the inner core of the tube, whereas a thermal boundary layer is formed near the tube wall. In the direction of the secondary flow, i.e., from $\theta = 0$ to $\theta = 180°$, the thermal boundary layer can be seen to grow in thickness. Also, the lower the Prandtl number, the thicker is the thermal boundary layer.

Local Heat Transfer Coefficient. The distribution of h_θ along the tube wall is determined by two factors: the variation of the axial velocity u_ϕ, and the thickness of the thermal boundary layer

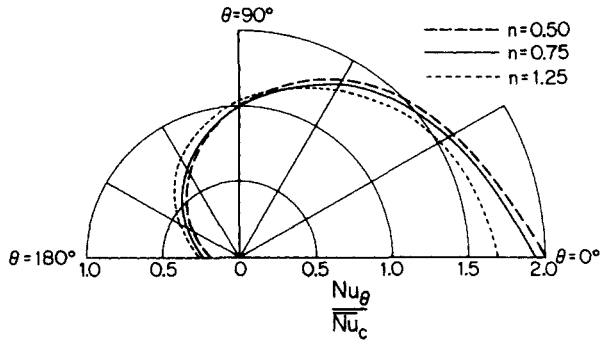

Figure 7. Circumferential variation of the local Nusselt number Nu_θ for different values of n at $De^+ = 700$, $Pr = 20$.

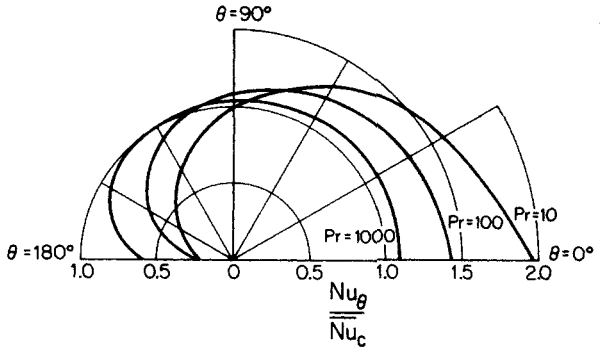

Figure 8. Circumferential variation of the local Nusselt number Nu_θ for different Prandtl numbers at $De^+ = 700$, $n = 0.75$.

created by the secondary flow. At $\theta = 0$, the combination of the largest axial velocity in the near-wall region and the thinnest thermal boundary layer is expected to lead to the highest heat transfer coefficient. This expectation is confirmed by the plots of $Nu_\theta/\overline{Nu}_c$ shown in Figures 7 and 8. As seen from Figure 7, the influence of n on the variation of the local heat transfer coefficient is not very significant at $De^+ = 700$; at lower Dean numbers, the influence of n is even weaker. The Prandtl number, on the other hand, is seen in Figure 8 to exert a substantial influence on the distribution of Nu_θ. For higher Prandtl numbers, the resistance to heat transfer is provided mainly by the thin thermal boundary layer, which is seen in Figure 6 to grow rather slowly. Consequently, the distribution of Nu_θ becomes more uniform as the Prandtl number increases.

Overall Heat Transfer Coefficient. Finally, the results for the overall Nusselt number $\overline{Nu}_c$ are presented in Figures 9 to 12 for various Prandtl numbers and for $n = 0.5$, 0.75, 1.0, and 1.25. These plots show the variation of the ratio $\overline{Nu}_c/\overline{Nu}_s$ with De^+. The value of $\overline{Nu}_s$ (the Nusselt number for a straight tube) is given in the caption of each figure for the corresponding value of n; incidentally, $\overline{Nu}_s$ does not depend on Pr. The increase of $\overline{Nu}_c$ with De^+ is to be attributed to the stronger secondary flow. Further, as expected on the basis of Eq. 25, the higher the Prandtl number, the greater is the benefit obtained from the secondary flow.

In any heat transfer enhancement device, the improved heat transfer coefficient is to be judged in conjunction with the unavoidable increase in the friction factor. For $De^+ = 1000$, the values

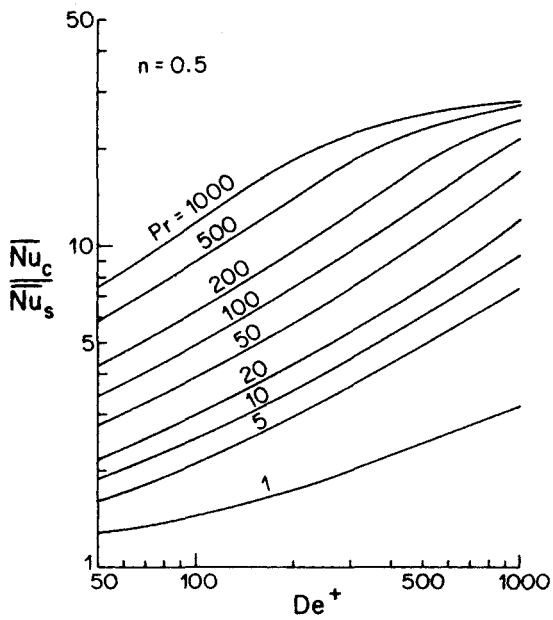

Figure 9. Variation of the average Nusselt number with modified Dean number for different Prandtl numbers and $n = 0.5$ ($\overline{Nu}_s = 4.746$).

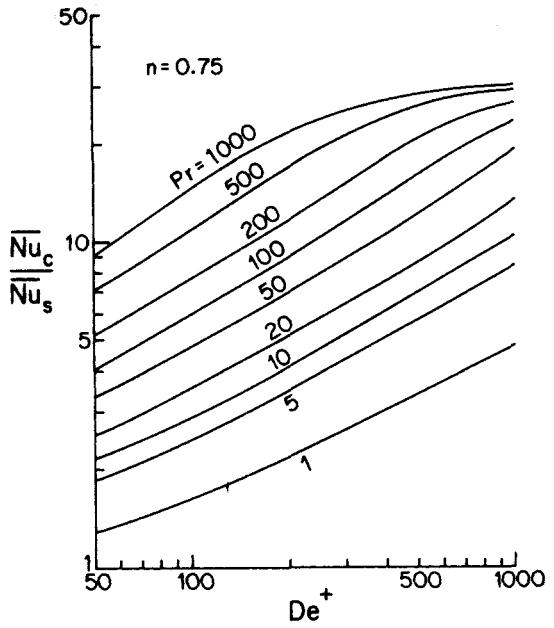

Figure 10. Variation of the average Nusselt number with the modified Dean number for different Prandtl numbers and n = 0.75 ($\overline{Nu}_s$ = 4.501).

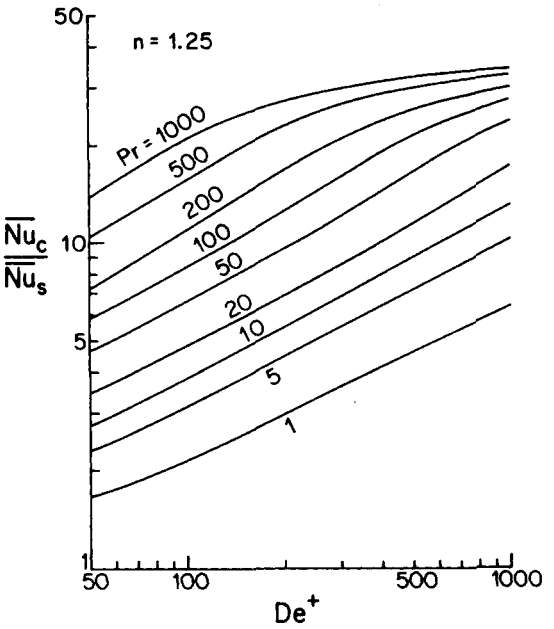

Figure 12. Variation of the average Nusselt number with the modified Dean number for different Prandtl numbers and n = 1.25 ($\overline{Nu}_s$ = 4.275).

of f_c/f_s (from Figure 4) range from 2.2 to 4.2 for the various values of n. The corresponding values of Nu_c/Nu_s can be seen to lie between 3.2 and 6.2 for Pr = 1; the heat transfer enhancement is even greater at higher Prandtl numbers. Thus, for the range of Pr and n considered in this study, the curved tube appears to be an attractive enhancement device for heat transfer.

Effect of Radius Ratio. The results presented so far are based on the assumption that the ratio a/R is small. This assumption has been used in obtaining the equations of motion, namely, Eqs. 2–5. Further, the neglect of the secondary velocities in Eq. 16, which gives the dimensionless viscosity M, is justified on the basis of small a/R. Thus, for a given fluid, De becomes the only governing parameter provided the ratio a/R is small. Otherwise, De and a/R (or Re and a/R) would have to be considered as two separate parameters.

In order to estimate the range of a/R values for which the present results are sufficiently accurate, a few calculations were performed with a more complete set of governing equations.

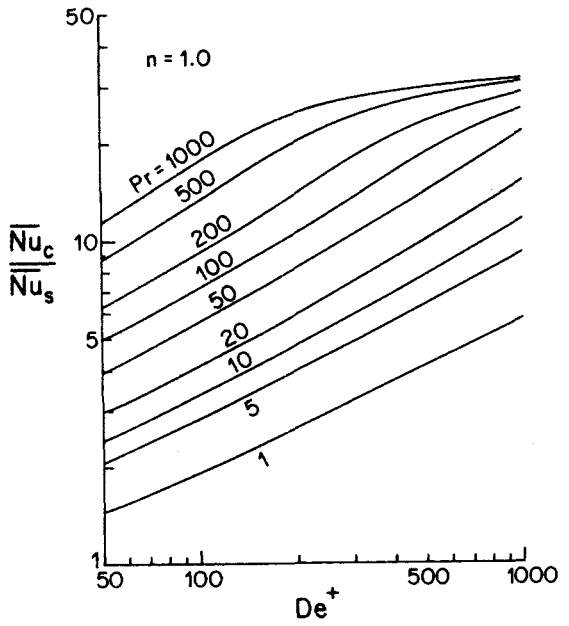

Figure 11. Variation of the average Nusselt number with the modified Dean number for different Prandtl numbers and n = 1. ($\overline{Nu}_s$ = 4.364).

First, the local radius of curvature was taken correctly as $R + r\cos\theta$, rather than simply R, in the momentum equations. The expression for M was as given by Eq. 16. The computed value of $f_c\mathrm{Re}^+$ changed by 1.5% for n = 0.5, De^+ = 700, and a/R = 0.1. When the equations of motion were taken from Eqs. 2–5, but the expression for μ was obtained from Eq. 14, the value of $f_c\mathrm{Re}^+$ for the same conditions changed by 1.2%.

It can, therefore, be concluded that the present results are sufficiently accurate for a/R values less than 0.1.

ACKNOWLEDGMENT

This research was performed under the auspices of NSF Grant NSF/CME 8007476.

NOTATION

a = radius of the tube
c_p = specific heat of the fluid
C = a constant, Eq. 19
d = diameter of the tube
D_{ij} = rate of strain tensor
De = Dean number, Eq. 9
De^+ = modified Dean number, Eq. 20
f_c = friction factor of the curved tube
f_s = friction factor of the straight tube
h_θ = local convective heat transfer coefficient
k = thermal conductivity of the fluid
K = consistency index
M = dimensionless viscosity, Eq. 1e
n = power-law index
$\underline{Nu}_\theta$ = local Nusselt number
$\overline{Nu}_c$ = average Nusselt number of the curved tube
$\overline{Nu}_s$ = average Nusselt number of the straight tube
p = pressure
P = dimensionless pressure, Eq. 1d
P_ϕ = pressure gradient, $-(1/R)(\partial p/\partial\phi)$
Pr = Prandtl number, Eq. 27
Q' = heat transfer rate per unit tube length
r = radial coordinate, Figure 1
R = radius of helix curvature
Re = Reynolds number, Eq. 10
Re^+ = modified Reynolds number, Eq. 18

S_{ci} = centrifugal source term in i momentum equation, $i = r, \theta$
S_{vi} = viscous source term in i momentum equation, $i = r, \theta$
T = temperature of the fluid
T_b = bulk temperature of the fluid
T_w = wall temperature
$\tilde{T}$ = dimensionless temperature, Eq. 24
$\tilde{T}_b$ = dimensionless form of T_b
u_i = velocity in i direction, $i = r, \theta, \phi$
$\bar{u}_\phi$ = average velocity in ϕ direction
$\bar{U}_\phi$ = dimensionless form of $\bar{u}_\phi$

Greek Letters

η = dimensionless radial coordinate, r/d
θ = angular coordinate, Figure 1
μ = apparent viscosity, Eq. 13
μ_{ref} = reference viscosity, Eq. 15
ρ = density of the fluid
ϕ = axial coordinate, Figure 1

LITERATURE CITED

Akiyama, M., and K. C. Cheng, "Boundary Vorticity Method for Laminar Forced Convection Heat Transfer in Curved Pipes," *Int. J. Heat Mass Transfer*, **14**, 1659 (1971).

Austin, L. R., and J. D. Seader, "Fully Developed Viscous Flow in Coiled Circular Pipes," *AIChE J.*, **19**, 85 (1973).

Dean, W. R., "Notes on the Motion of Fluid in a Curved Pipe," *Phil. Mag.*, **4**, 208 (1927).

Ito, H., "Laminar Flow in Curved Pipes," *Inst. High Speed Mech.*, Japan, **22**, 161 (1970).

Gupta, S. N., and P. Mishra, "Isothermal Laminar Flow of Non-Newtonian Fluids through Helical Coils," *Indian J. of Technology*, **13**, 245 (1975).

Mashelkar, R. A., and G. V. Devarajan, "Secondary Flow of Non-Newtonian Fluids: Part I—Laminar Boundary Layer Flow of a Generalized Non-Newtonian Fluid in a Coiled Tube," *Trans. Instn. Chem. Engrs.*, **54**, 100 (1976a).

Mashelkar, R. A., and G. V. Devarajan, "Secondary Flow of Non-Newtonian Fluids: Part II—Frictional Losses in Laminar Flow of Purely Viscous and Viscoelastic Fluids through Coiled Tubes," *Trans. Instn. Chem. Engr.*, **54**, 108 (1976b).

McConalogue, D. J., and R. S. Srivastava, "Motion of Fluid in a Curved Tube," *Proc. Royal Soc.*, **A307**, 37 (1968).

Mori, Y., and W. Nakayama, "Study on Forced Convective Heat Transfer in Curved Pipes," *Int. J. Heat Mass Transfer*, **8**, 67 (1965).

Mujawar, B. A., and M. R. Rao, "Flow of Non-Newtonian Fluids through Helical Coils," *Ind. Eng. Chem. Process Des. Dev.*, **17**, 22 (1978).

Patanakar, S. V., V. S. Pratap, and D. B. Spalding, "Prediction of Laminar Flow and Heat Transfer in Helical Coiled Pipes," *J. Fluid, Mech.*, **62**, 539 (1974).

Patankar, S. V., *Numerical Heat Transfer and Fluid Flow*, McGraw-Hill, New York (1980).

Rajasekharan, S., V. G. Kubair, and N. R. Kuloor, "Flow of Non-Newtonian Fluid through Helical Coils," *Indian J. of Technology*, **8**, 391 (1970).

Topakoglu, H. C., "Steady Laminar Flow of an Incompressible Viscous Fluid in Curved Pipes," *J. Math. Mech.*, **16**, 1321 (1967).

Truesdell, L. C., Jr., and R. J. Adler, "Numerical Treatment of Fully Developed Laminar Flow in Helical Coiled Tubes," *AIChE J.*, **16**, 1010 (1970).

Manuscript received May 11, 1981; revision received September 14, and accepted October 9, 1981.

Multiparameter Corresponding-States Correlation of Coal-Fluid Thermodynamic Properties

A multiparameter corresponding-states correlation has been developed to describe fossil-fluid thermodynamic properties needed to design fluid-flow, heat-exchange, and other unit operations in coal-liquefaction plants. Three equation-of-state parameters, a molecular-size/separation parameter, a molecular-energy parameter, and a molecular-orientation parameter are used to characterize nonpolar and slightly polar aromatic hydrocarbons. A conformal-solution model is developed for predicting thermodynamic properties of coal-derived mixtures.

M. R. BRULÉ, C. T. LIN, L. L. LEE, and K. E. STARLING

University of Oklahoma, Norman, OK

SCOPE

The objective of this work was to develop first-generation methodologies for predicting thermodynamic properties of coal-derived fluids using current equation-of-state technology. Previously, most equations of state could not be applied directly to coal fluids. A corresponding-states framework has been modified to rapidly develop practical properties-prediction capability for the coal pilot- and demonstration-plant programs.

The three-parameter corresponding-states correlation presented here is shown to accurately describe the thermodynamic behavior of many pure coal chemicals and the bulk thermodynamic properties of undefined distillable coal fractions. The vapor/liquid equilibrium of both defined and complex distillable mixtures can be predicted using a conformal-solution model (Watanasiri et al., 1981).

Characterization techniques are outlined for converting analyses of undefined mixtures (with composition available in terms of broad fractions) into representative pseudocomponents. Empirical correlations have been developed to estimate pseudocomponent characterization parameters and ideal-gas thermodynamic properties for use with the equation of state.

Correspondence concerning this paper should be addressed to M. R. Brulé who is presently with Kerr-McGee Corp., Oklahoma City, OK.

C. T. Lin is presently with Bechtel National, Inc., Houston, TX.

K. E. Starling is the principal investigator.

0001-1541-82-4018-0616-$2.00.